to be

$$U_\infty = -\frac{\partial\sigma}{\partial T}\frac{q''\alpha R_0}{k_2}\frac{1}{3\mu_2}\frac{1}{(K+2)(2+3X)} \quad (20)$$

where μ_2 is the dynamic viscosity of the continuous phase, and X is the ratio of viscosities (droplet to continuous phase). The stream function values (made dimensionless by $U_\infty R_0^2$) are obtained from equations (12) and (13) of Levan

$$\psi_1 = \frac{-3}{4}(r^2-r^4)\sin^2\theta + \sum_{\substack{n=3\\(\text{odd})}}^{\infty}\frac{3n(n-1)(2+3X)(K+2)}{2(2n-1)(1+X)} \times a_{n-1}(r^{2+n}-r^n)C_n^{-1/2}(\cos\theta) \quad (21)$$

$$\psi_2 = (r^2-r^{-1})\frac{\sin^2\theta}{2} + \sum_{\substack{n=3\\(\text{odd})}}^{\infty}\frac{3n(n-1)(2+3X)(K+2)}{2(2n-1)(1+X)} \times a_{n-1}(r^{3-n}-r^{1-n})C_n^{-1/2}(\cos\theta) \quad (22)$$

with

$$u = \frac{-1}{r^2\sin\theta}\frac{\partial\psi}{\partial\theta}, \quad v = \frac{1}{r\sin\theta}\frac{\partial\psi}{\partial r}. \quad (23)$$

3. DISCUSSION

The bulk droplet velocity predicted by equation (20) is much smaller than that which would be significant in most buoyancy driven flows in the earth's gravitational field. However, surface tension driven velocities could be significant in a micro-gravity environment. The flow lines inside and near such a droplet are illustrated in Fig. 2, for the special case where the ratio of viscosities and thermal conductivities are unity (i.e. $X = 1$, $K = 1$).

Perhaps the most restrictive of the assumptions made in the preceding analysis is assumption (5), the assumption that the droplet surface acts as a gray body to the incident irradiant energy. Most droplets will be semi-transparent to irradiant energy in the visible range. Thus the preceding analysis is strictly valid for only a few systems. However, if the droplet absorbs a significant amount of the incident irradiant energy, the droplet will have a non-uniform temperature profile which can induce droplet motion resulting from gradients in the interfacial surface tension. The bulk droplet velocity for such a semi-transparent droplet is expected to be smaller, yet qualitatively similar to that predicted by equation (20).

REFERENCES

1. M. D. Levan, Motion of a droplet with a Newtonian interface, *J. Colloid Interface Sci.* **83**(3), 11–17 (1980).
2. R. L. Thompson, K. J. DeWitt and T. L. Labus, Marangoni bubble motion phenomenon in zero gravity, *Chem. Engng Commun.* **5**, 299–314 (1980).
3. V. Ya. Rivkind and G. S. Sigovtsev, Motion of a droplet in a nonisothermal flow, *Fluid Mech.—Sov. Res.* **10**(1), 36–46 (1981).
4. J. D. Talman, *Special Functions*, Chap. 9. W. A. Benjamin, Menlo Park, California (1968).

Int. J. Heat Mass Transfer. Vol. 31, No. 7, pp. 1537–1539, 1988
Printed in Great Britain

0017-9310/88 $3.00+0.00
Pergamon Press plc

Radiation configuration factors from axisymmetric bodies to plane surfaces

M. H. N. NARAGHI
Department of Mechanical Engineering, Manhattan College, Riverdale, NY 10471, U.S.A.

and

J. P. WARNA
Department of Chemical Engineering, University of Abo Akademi, Turku, Finland

(*Received* 28 *September* 1987 *and in final form* 19 *January* 1988)

INTRODUCTION

A LARGE number of view factors between a variety of surfaces has been evaluated using different numerical and analytical methods [1]. A close examination of the literature reveals that little work has been done on the view factors between axisymmetric bodies and plane surfaces. This note develops a general formulation for evaluating the view factors between axisymmetric bodies and plane surfaces perpendicular to the axis of symmetry.

FORMULATION

Consider the configuration shown in Fig. 1, consisting of an axisymmetric body and a plane surface perpendicular to the axis of symmetry. The view factor from differential areas to most commonly used axisymmetric bodies are known, e.g. the view factors from a differential area to a disk [2], a cylinder [3], a cone [4, 5], a sphere [6, 7] and a spherical segment [8].

A differential ring sector can be generated by rotating the differential area about the axis of symmetry as shown in Fig. 1. Note that the angle of rotation is ϕ. Thus, the view factor from the axisymmetric body to the planar surface can be determined by integrating the view factor from the axisymmetric body to the differential ring over the area of the planar surface

$$F_{Ax-A} = \int_{a_1}^{a_2} \mathrm{d}F_{Ax-\delta r} \quad (1)$$

where

$$\mathrm{d}F_{Ax-\delta r} = \phi\frac{\mathrm{d}F_{Ax-\mathrm{d}A}}{\mathrm{d}\phi} = \phi F_{\mathrm{d}A-Ax}\frac{\mathrm{d}A/\mathrm{d}\phi}{Ax} \quad (2)$$

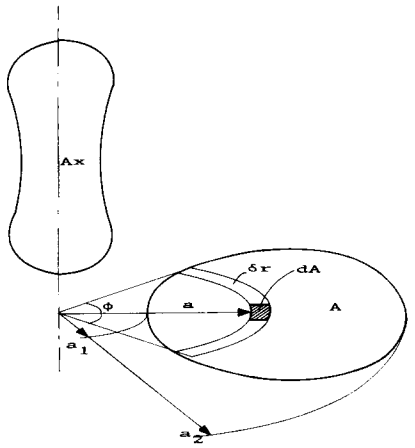

FIG. 1. Axisymmetric body and plane surface configuration.

and ϕ is a function representing the contour of plane surface A in a polar coordinate system the center of which is the intersection of the axis of symmetry and the planar surface. Thus, equation (1) becomes

$$F_{Ax-A} = \frac{1}{Ax}\int_{a_1}^{a_2} \phi(a) F_{dA-Ax}\, a\, da. \tag{3}$$

For circles the function $\phi(a)$ is given by

$$\phi(a) = \cos^{-1}\left(\frac{a^2+a_0^2-r^2}{2aa_0}\right) \tag{4}$$

where r is the radius of the circle and a_0 the radial coordinate of its center. Limits of integrations a_1 and a_2 for this case are: $a_1 = a_0 - r$ and $a_2 = a_0 + r$. Note that $\phi(a)$ given by equation (4) corresponds to a half circle, and the view factor to a disk is twice that obtained based on equations (3) and (4).

For a straight line connecting points 1 and 2, $\phi(a)$ is given by

$$\phi(a) = \sin^{-1}\left[\frac{y_1(x_2-x_1)-(y_2-y_1)x_1}{a(x_2-x_1)}\cos\beta\right] + \beta \tag{5}$$

where

$$\beta = \tan^{-1}\left(\frac{y_2-y_1}{x_2-x_1}\right)$$

(x_1, y_1) and (x_2, y_2) are coordinates of points 1 and 2 in the Cartesian coordinate system and β is the angle of the line with the x-axis. When $x_1 = x_2$, $\phi(a)$ for the straight line becomes

$$\phi(a) = \cos^{-1}\left(\frac{x_1}{a}\right). \tag{6}$$

APPLICATIONS

Considering the view factors from a disk to another disk, $\phi(a)$ is given by equation (4). Figure 2 shows the resulting view factors vs h/r_1 and a_0/r_1 as a parameter when $r_2/r_1 = 1$. Note that when $a_0 = 0$ the resulting view factors are identical to those of the exact solution given in ref. [1].

Another case is the view factor from a disk to a disk segment. The contour of a disk segment consists of a circle part and a straight line part. For the circle part equation (4) and for the straight line part equation (5) are used for $\phi(a)$ in equation (3). Figure 3 shows the resulting view factors from disks to disk segments.

For a limiting case when the two disks are coaxial the results produced by the present method are identical to those

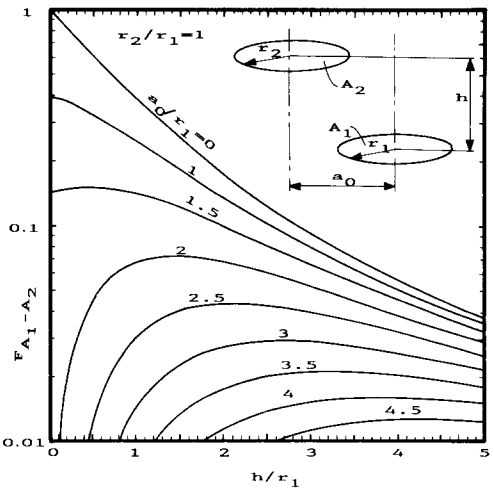

FIG. 2. View factor between two parallel non-coaxial disks.

given in ref. [9]. However, it is worth mentioning that the formulation given by equation (3) requires one numerical integration, while the formulation described in ref. [9] involves two numerical integrations. Furthermore, the present formulation is more versatile than the formulation given in ref. [8] and can be used to evaluate view factors for non-coaxial cases and more diversified configurations.

Next, consideration is given to the view factor from a disk to a polygon. The sides of the polygon consist of straight lines; hence, equations (5) and (6) can be used to determine $\phi(a)$. In this case, equation (3) has to be evaluated for each side of the polygon and the resulting equation is in the form of a finite series which is given by

$$F_{Ax-\text{Polygon}} = \frac{1}{Ax}\sum_{n=1}^{m}\int_{a_n}^{a_{n+1}} \phi(a) F_{dA-Ax}\, a\, da \tag{7}$$

where $a_n = \sqrt{(x_n^2+y_n^2)}$ and, x_n and y_n are coordinates of vertex n of the polygon in the Cartesian coordinate system, $a_1 = a_{m+1}$ and m is the total number of vertices. Note that the order of numbering of the vertices should be clockwise when they are in the first or third quadrant and counter-clockwise when they are in the second or fourth quadrant in order to obtain positive view factors.

If the function representing the contour of the plane surface is not known in an algebraic form, the contour can be

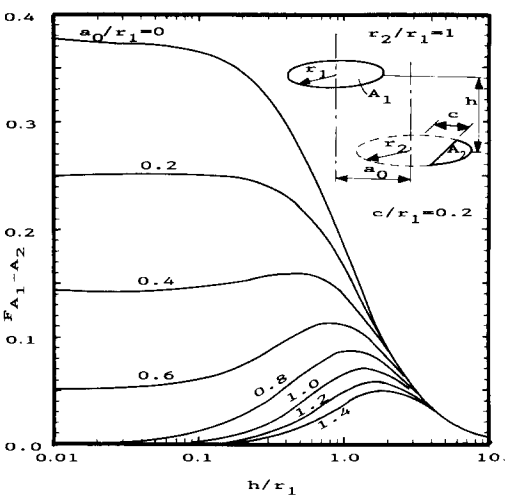

FIG. 3. View factor between a disk and a disk segment.

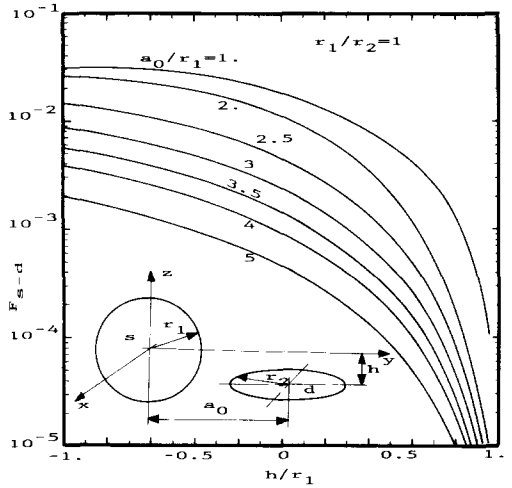

FIG. 4. View factor between a sphere and a non-coaxial, intersecting disk.

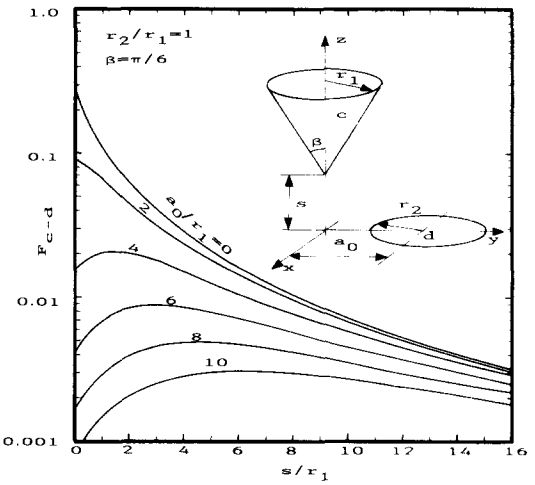

FIG. 6. View factor between a cone and a disk.

represented by a number of discrete points and the surface can be approximated by a polygon with the discrete points as its vertices. Equation (7) can then be used to determine the view factor from the disk to the surface. The accuracy of this approach was tested using the view factors between two disks by approximating one of the disks as a polygon with eight vertices and comparing the results to the exact solution given in ref. [1]. The results agree to four or more decimal points.

Another configuration which was studied is the sphere and plane surface configuration. The view factor from spheres to non-coaxial and non-intersecting disks have been evaluated by Feingold and Gupta [10]. The results of the present formulation for the view factor between spheres and non-intersecting disks are found to be in agreement with those of ref. [10]. The resulting view factors from spheres to non-coaxial and intersecting disks are shown in Fig. 4. These results are from the whole sphere to the upper part of the disk.

Next, the view factor from cones and cylinders to planar surfaces is considered. Making use of the view factor from a differential area to a cylinder given in ref. [3] and equation (3), the view factors from cylinders to planar surfaces can be calculated. Figure 5 shows the view factor from a cylinder to a non-coaxial disk. Similarly, the view factor from cones to plane surfaces can be calculated by making use of the view

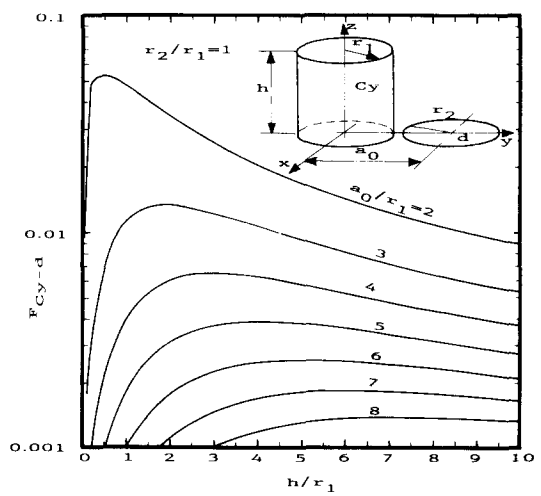

FIG. 5. View factor between a cylinder and a disk.

factor from a differential area to a cone given in refs. [4, 5], and equation (3). Figure 6 shows the view factors from cones to non-coaxial disks.

In summary, the method discussed in this note can be used to evaluate radiative configuration factors from axisymmetric bodies and plane surfaces. The present approach (equation (3)) requires the view factor from differential areas to the axisymmetric body which is known for most common axisymmetric bodies, and a function representing the contour of the plane surface in a polar coordinate system. If this function is not known in algebraic form, then it can be approximated by a set of discrete points, and equation (7) used to evaluate the view factor.

REFERENCES

1. J. R. Howell, *A Catalogue of Radiation Configuration Factors*. McGraw-Hill, New York (1982).
2. M. H. N. Naraghi, Radiation view factors from differential plane sources to disks—a general formulation, *AIAA J. Thermophys. Heat Transfer* (1988), in press.
3. E. M. Sparrow, G. B. Miller and V. K. Jonsson, Radiating effectiveness of annular-finned space radiators, including mutual irradiation between radiator elements, *J. Aerospace Sci.* **29**(11), 1291–1299 (1962).
4. C. P. Minning, Calculation of shape factors between rings and inverted cones sharing a common axis, *Trans. ASME J. Heat Transfer* **99**, 492–494 (1977).
5. B. T. F. Chung, M. M. Kermani and M. H. N. Naraghi, A formulation of radiation view factors from conical surfaces, *AIAA J.* **22**(3), 429–436 (1984).
6. N. H. Juul, Diffuse radiation view factors from differential plane sources to spheres, *Trans. ASME J. Heat Transfer* **101**, 558–560 (1979).
7. B. T. F. Chung and M. H. N. Naraghi, A simpler formulation for radiative view factors from spheres to a class of axisymmetric bodies, *Trans. ASME J. Heat Transfer* **104**, 201–204 (1982).
8. M. H. N. Naraghi, Radiative view factors from spherical segments to planar surfaces, *AIAA J. Thermophys. Heat Transfer* (1988), in press.
9. S. Lin, P.-M. Lee, J. C. Y. Wang, W.-L. Dai and Y.-S. Lou, Radiant-interchange configuration factors between disk and a segment of parallel concentric disk, *Int. J. Heat Mass Transfer* **29**, 501–503 (1986).
10. A. Feingold and K. G. Gupta, New analytical approach to the evaluation of configuration factors in radiation from spheres and infinitely long cylinders, *Trans. ASME J. Heat Transfer* **92**, 69–76 (1970).